The Influence of Salinity, pH, Temperature and Particles on Produced Water Oil Quantification Precision and Accuracy with Confocal Laser Fluorescence Microscopy

*Jingjing Fan[1], Stacey Louie[1], Debora F. Rodrigues[1]**

1 Department of Civil and Department of Environmental Engineering, University of Houston, Houston, TX 77204-4003

* **Corresponding authors:** dfrigirodrigues@uh.edu, phone: 713-743-1495; Rifai@uh.edu; phone: 713-743-4271.

Abstract

The present study investigates the effects of different produced water parameters, e.g. salinity, pH, temperature and presence of colloidal particles, in oil quantification using confocal laser fluorescence microscopy (CLFM). The study simulates different produced water samples, which typically contains a mixture of oil, salts, and different concentrations of particles. The results showed that under extreme environmental conditions, i.e. high pH (pH 8), salinity (250000 ppm) and temperatures (60 ºC), the CLFM oil quantification precision was reduced. The accuracy of the quantification, on the other hand, was not affected by the environmental condition for all the conditions investigated. Average oil droplet size and oil-water emulsion polydispersity have great correlation with CLFM measurement precision. Interfacial tension and DLVO interactions were employed to gain a better mechanistic understanding of how the environmental conditions affect the size or colloidal stability of the oil droplets and therefore impact the precision of CLFM measurements. To understand the relationship of different environmental parameters with the level of CLFM measurement precision, multiple correspondence analysis (MCA) was employed. The results showed that conditions of lower salinity, temperature, and SiO_2 concentration, as well as neutral pH (pH 7), favor smaller oil droplet sizes in the oil-in-water emulsion and more precise CLFM measurements. The better understanding of the impact of different water chemistries in oil droplet stability will be essential for decision makers on conditions that could impact the accuracy of the method. This work presents a new perspective of investigating oil in water analysis technology and guide engineers operating novel technologies in their optimum environmental conditions and achieving the best performance of the technology.

Graphical Abstract

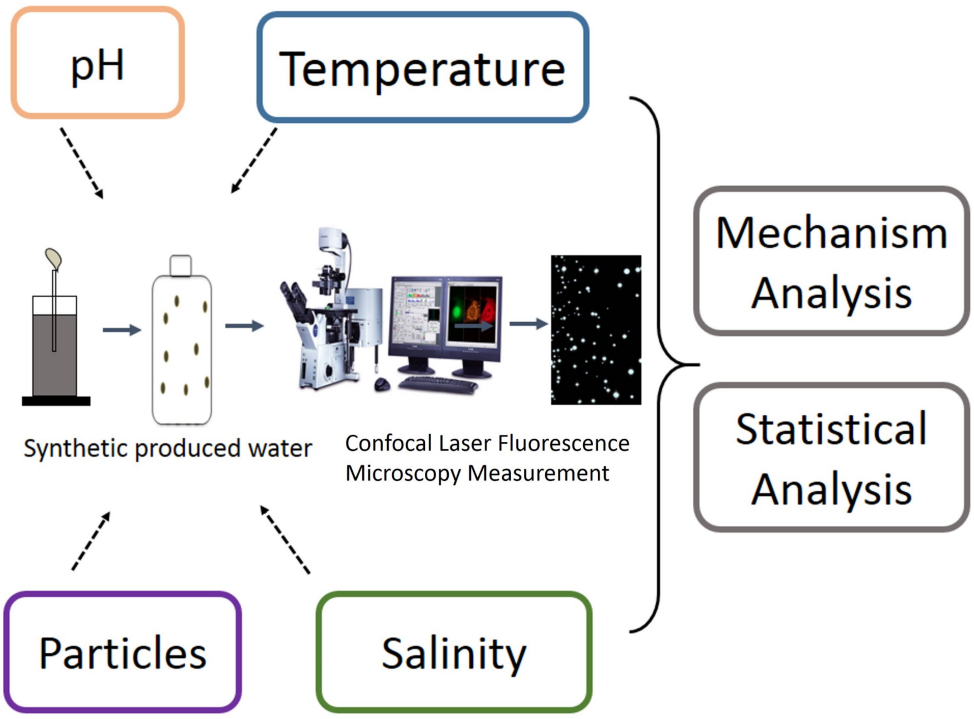

Key words: confocal microscope, oil, salinity, particles, DLVO

Introduction

Offshore oil and gas activities have been established over the past 50 years. Nowadays, more than 65 oil and gas producing fields are in operation, and the number is still increasing.[1] Most potential environmental impacts related to oil and gas industry activities are the pollution brought by hydrocarbons of petroleum throughout all stages of oil and gas production, i.e. from exploratory activities to refining.[2] In general, oil pollution originated from these activities comes from damaging pipelines and decreasing efficiency of wastewater treatment. This type of pollution can endanger organisms' health and disrupt environmental balance.[3]

By far, produced water is the major source of hydrocarbon contamination entering the sea from regular operatio.[4] Therefore, regulations set strict limitations on levels of oil and grease that can be discharged to the sea for these types of wastewater. Several methods have been established for oil and grease quantification for produced water discharge. The most widely used is the EPA 1664 method. This method is expensive and labor intensive due to the requirement of large laboratory space, specialized equipment and well-trained personnel to perform the analysis.[5] The limitations of the EPA method led to the development and optimization of alternative methods, such as the infrared (IR) and gas chromatography (GC) methods. However, these methods cannot obtain real-time measurements.[6] Therefore, other inexpensive, reliable, and rapid methods to determine oil and grease concentrations in water samples are still of great need.

Recently, the confocal laser fluorescence microscope (CLFM) was shown to be able to quantify oil concentrations by measuring the fluorescent signals in 3D images.[7] Due to its high sensitivity, good diagnostic potential, relatively simple instrumentation and suitability for either laboratory-based

or portable instrumentation, this method was suggested to have great potential to be used for real-time oil quantification in subsea systems.

So far, all the CLFM measurement investigations were performed under relatively simple systems (zero salinity, neutral pH, room temperature and no particles).[7] In real environmental discharge, the physical and chemical properties of produced water vary considerably depending on the geographic location of the field, the geological formation, the type of hydrocarbon being produced and the treatment applied before discharge. Diverse studies have suggested that increasing salinity in aqueous phase would destabilize the oil/water emulsion, and then increase observed oil droplet size under the microscope.[8, 9] The pH would also alter the surface charge of the emulsion, which could lead to changes in the oil droplet size over time.[10] Also, temperature could affect the collision velocity of oil droplets and particles leading to larger aggregates. All these parameters might interfere with the oil droplet quantification with microscopy techniques, such as CLFM.[11, 12] However, detailed investigations of how these environmental parameters can affect CLFM measurements have not been fully assessed. Thus, produced water containing various concentrations of salts, various pH, different temperature and particle concentrations need to be investigated to determine the suitability of this new method for a wide range of produced water that could be generated in different production sites.

In this study, synthetic produced water samples prepared with different types of oil samples at various concentrations were investigated under different environmental parameters, i.e. salinity, pH, temperature, and particles to determine the effects of these parameters in oil quantification using the CLFM method. The range of salinity, pH, temperature, and particle concentrations (SiO_2) of the synthetic produced water in this study were based on various reported real produced water discharge properties (0 – 250,000 ppm of salinity, 3 – 8 pH, 4ºC to 60 ºC and 0 – 50 ppm SiO_2).[2, 6, 13, 14] The mechanisms which led to more or less precise CLFM measurements were evaluated through zeta

potential, surface/interfacial tension measurement, and Laplace pressure. The DLVO theory was also employed to better understand the interactions of the particles with oil in the produced water. Multiple correspondence analysis and multivariate regression analysis were applied to predict the level of precision of CLFM measurements under combined complex environmental conditions.

Material and Methods

1. Synthetic Produced Water Preparation with different environmental parameters

Two oil samples were provided by Clearview Subsea Inc. with an API (American Petroleum Institute) of 24.3 (specific gravity of 0.908 g/mL), and API of 36.3 (specific gravity of 0.843 g/mL), respectively. They were used to prepare the concentrations of 25 ppm and 50 ppm of synthetic produced water samples for the present study. During the sample preparation, control solutions were prepared with oil and nanopure water (Thermolyne Nanopure lab water system) at pH 7, salinity 0 ppm at room temperature (25 ºC). The tested solutions under different conditions contained different salinity, pH, temperatures and particle concentrations. More specifically, saline water containing concentrations at 35,000 ppm, 100,000 ppm and 250,000 ppm of NaCl (ACS reagent, >99.0%, Sigma-Aldrich) was prepared to investigate the impact of salinity; while the pH of water was adjusted at 3, 4, 5, 6, and 8 using 1M HCl and 1M NaOH to determine the influence of pH toward the accuracy and precision of the CLFM method. The effects of different temperatures on CLFM detection were determined at 4ºC, 25ºC, and 60ºC by keeping the nanopure water at 4ºC in the refrigerator, room temperature and 60ºC water bath overnight and during sample analysis. The concentration of SiO_2 (99%, particle size between 0.5- 10 µm, approx. 80% between 1-5 µm, Sigma Aldrich) at 25 ppm and 50 ppm were prepared to investigate the influence of particles on the CLFM method. In this study, 25 ppm and 50 ppm of two types of synthetic produced water were prepared to encompass the range

of EPA regulated discharge concentration of produced water, which is 42 ppm as a maximum daily value and 29 ppm as a monthly average.[6]

2. CLFM set up and experimental parameters

After sample preparation, a disperser (T 18 Digital ULTRA-TURRAX Disperser, IKA INDIA) was used to mix the sample at 10,000 rpm for 3 min vigorously. In order to avoid the temperature change during the sample dispersing, the sample bottles at 4°C and 60°C were kept in an ice bath and a hot bath, respectively. After mixing, the temperature was monitored again using a thermometer (Lab thermometer, temperature range: between -20 and 110 °C). A homogeneous solution was generated through mixing, and then 200 µL of each sample was taken from the sample bottle and injected into a flow cell (µ-Slide I 0.8 Luer Collagen IV: #1.5 polymer coverslip, sterilized, ibidi). The flow cell with synthetic produced water sample was placed on the top of a sample holder and analyzed using CLFM (Leica DM2500B SPE, Lasertechnik, Heidelberg, Germany). The oil droplets in the sample were observed using 10X objective lens with 488 nm excitation wavelength, while the emission signals were collected from wavelength 500 to 600 nm. In all experiments, each stack of image was acquired with a total thickness of 500 µm at intervals of 4 µm for each slice of the image from the top to the bottom of the flow cell. A total of three stack images of each sample was analyzed at random positions of the flow cell, and the same procedure was repeated three times for the water taken from the top, medium, and bottom of the same sample bottle. Thus, a total of nine stacks for each sample was used for statistical analysis.[7]

Afterward, the concentration of oil content in synthetic produced water was calculated through Matlab with the global thresholding procedure. The detailed image analysis steps were described in our previously published study.[7] Briefly, the optimum threshold was selected through calibration from different concentrations of synthetic produced water, and then the white oil droplets on a black

background were calculated using the volume of white pixels showed in the images. In this study, all the images were analyzed with the optimum threshold (0.5) as previously determined.[7]

3. Oil Property Investigation

In order to understand the oil droplet changes under various environmental condition, pure oil samples and oil/water mixtures under different conditions were investigated. For pure oil samples, total acid number and total base number which are important parameters for oil property were tested. For oil/water mixture under environmental conditions, surface tension, interfacial tension, zeta potential and particle sizes were investigated.

3.1 Pure oil sample analysis – total acid number and total base number determination

Individual Dexsil Titra-Lube TAN and TBN kits (Dexsil Corporation, U.S) were used to determine the total acid number and total base number in the oil samples. Briefly, 2mL of sample oil was taken and mixed with isooctane. By adding a predetermined amount of acidic species (isopropyl HCl) to the sample, any basic species contained in the oil sample would react with known concentrations of acidic species. A total volume of 7 mL of aqueous solution were shaken vigorously for 30 s and let stand upside down to allow the phases to separate for 3 min in the tube. This allowed the remaining acidic species to be extracted into an extractant phase, and then separated from the oil sample. Five mL of an aqueous phase containing the residual acidic species were then transferred to a fresh tube for colorimetric titration. The total base number was determined by measuring the remaining acidic species in the extractant phase through a colorimetric titration of KOH.[15] The TBN number of the oil sample was determined by titration. A similar procedure was used for TAN determination, where isopropyl KOH and HCl were used as predetermined basic species and the titrating solution, respectively.

3.2 Investigation of Oil Droplet Properties under Different Environmental Conditions

In order to understand how the environmental parameters affect the oil droplets in water which in turn influence the CLFM measurements, different investigations were conducted including surface tension, interfacial tension, zeta potential, and particle size.

3.2.1. Surface tension and Interfacial Tension Measurements

Surface tension and interfacial tension are important factors in the formation and stability of fluid system such as emulsions.[16] The surface tension and interfacial tension measurements were done using a CENCO DuNouy tensiometer (Central Scientific Co. Chicago) according to the ASTM standards D 1331.[17] For surface tension, 100 mL solution containing various environmental factor (pH, temperature, salinity, and particles) was poured into a clean 90 mm diameter crystallizing dish (Kimax glass crystallizing dish, 90 mm diameter, UNSPSC Codes: 41121812) and then the sample was placed on the sample platform. After setting the dial to zero, the sample platform was raised until complete submersion of the platinum ring occurred into the sample. By adjusting the dial-adjusting screw, a torsion was applied to the wire ring, leading to detachment of the ring from the solution surface. The surface tension value was recorded when the ring broke free from the solution. For the interfacial tension, 50 mL of water under different conditions (salinity, pH, temperature, and particle concentration) were poured into the clean dish. The platform where the sample located was raised until the ring was immersed from 5 to 7 mm in the water sample. The oil sample was then poured on the water with a thickness of 5 mm to 10 mm. The dish was adjusted to a position where the ring was in the interface between the water and the oil. A torsion was applied by adjusting the dial-adjusting screw. The interfacial tension reading was determined when the film at the interface broke. Three

measurements were obtained for each sample. The surface tension and interfacial tension values were measured with an accuracy of 0.1 dyn/cm.[17]

3.2.2 Zeta potential and particle size measurements

Zeta potential and particle size measurements were investigated for two synthetic produced water with different API values with pH values ranging between 3 to 8 and SiO_2 concentrations of 25 ppm and 50 ppm. Zeta potential measurements for synthetic produced water under various pH were done with freshly prepared and dispersed samples, as well as samples settled for 10 min. The selection of 10 min settling time was to keep consistent with the time usually taken for the CLFM measurements for the triplicate measurements. All the samples for zeta potential and particle size measurements contained 10 mM of NaCl as an inert supporting monovalent electrolyte to preserve the sample stability.[18] The samples were injected into a capillary cell (disposable folded capillary cell, Fisher Scientific) with a syringe. The cell was held up-side-down during injection until it was half-full and then turned back up for further injection in order to avoid air bubbles in the cell. After that, the cell was placed in a Dynamic light scattering (DLS) instrument (Nicomp 380 DLS/ZLS, Particle Sizing Systems). The zeta cell (disposable cuvettes, Fisher Scientific) with 1 mL of sample was used for particle size measurements.

3.2.3 Interaction Potential Investigation

In this study, three different interactions were taken into account: interactions between silica particles, between one silica particle and one oil droplet, and between two oil droplets. All these interactions are described by the classical DLVO potential.[19] The total energies were calculated as the summation of van der Waals (V_A) and electrostatic double layer (V_R) interaction based on the following equations.

$$V_A = -\frac{A_H a_1 a_2}{6h(a_1+a_2)(1+\frac{14S}{\lambda})} \quad (1)$$

$$V_R = 64\pi\varepsilon_0\varepsilon_r \frac{a_1 a_2}{a_1+a_2} \left(\frac{K_B T}{ze}\right)^2 \left[\tanh\left(\frac{z\widetilde{\psi_1}}{4}\right)\right]\left[\tanh\left(\frac{z\widetilde{\psi_{21}}}{4}\right)\right]\exp(-\kappa s) \quad (2)$$

$$\kappa = \left(\frac{2e^2 I N_A}{\varepsilon_0\varepsilon_r K_B T}\right)^{1/2} \quad (3)$$

$$I = \frac{1}{2}\sum c_i z_i^2 \quad (4)$$

$$\tilde{\psi} = e\psi/K_B T \quad (5)$$

Where A_H is Hamaker constant, S is the separation distance between particle centers, λ is the "characteristic wavelength" of the interaction, often assumed to be 100 nm. and a_1, a_2 are the particle radius determined through particle size measurement.[20] K_B is Boltzmann's constant (1.3807×10^{-23} J/K), ε_0 is permittivity of free space (8.85×10^{-12} C^2/J m), ε_r represents the relative permittivity dielectric constant of water (75.8), and e is the electron charge (1.602×10^{-19} C)., and N_A is Avogadro's number (6.022×10^{23} mol^{-1}) in equation 3. In equation 4. I is ionic strength, ci is the molar concentration of ion Na^+, and Cl^- (mol/L) in this study, and Zi is the charge number of the ion (which equal to +1 and -1 in this study). The value of ψ_1 and ψ_2 are the zeta potential values determined through zeta potential measurement and $\tilde{\psi}$ was calculated through equation 5. The Hamaker constants for SiO_2-SiO_2, SiO_2 and oil droplets, and oil-oil interactions are 2.4×10^{-21} J, 8.5×10^{-21} J, and 1×10^{-20} J, respectively. [21-23]

4 Statistical Analysis

For all set of experiments, at least three replicate samples were conducted to take into consideration reproducibility. The averages, standard deviations, and histograms were calculated with Excel. In this

study, the accuracy of the CLFM method was calculated from Equation 6, and precision of each CLFM detection was calculated with Equation 7. The equations are defined in the EPA 1664 standard method.[24]

$$x = \frac{Measured\ concentration}{Prepared\ concentration} \times 100\% \quad (6)$$

$$s = \sqrt{\frac{\sum x^2 - \frac{(\sum x)^2}{n}}{n-1}} \quad (7)$$

where:

x= Detection accuracy

s = Sample precision

n= Number of samples

The measurements for each sample were checked for outliers. The outliers were determined based on the interquartile (IQR) range of the dataset. The IQR equals the values between the first and third quartile. Any data point that lies 1.5 times IQR below the first quartile or 1.5 times IQR above the third quartile was considered an outlier. The outliers were not considered in the calculations and whenever necessary the experiment was repeated.

Spearman's rank correlation coefficient was computed by excel and used to assess the relationship between different variables including CLFM measurement precision, average oil droplet size, and polydispersity. Multiple correspondence analysis (MCA) was employed to investigate the relationship between the precision level with different environmental factors. The MCA was done using XLSTAT statistical software in Excel (Addinsoft). To perform this procedure, all the precision obtained from CLFM analysis under different environmental conditions (pH, salinity, temperature, particle concentration) were ranked from smallest to largest. Any precision data smaller than 20%

was defined as Precision -High, while the precision values between 20% - 30%, and higher than 30% were categorized as Precision-Medium and Precision-Low, respectively. The MCA was used to correlate the environmental factors to the level of CLFM measurement precision. For the MCA, a disjunctive table was generated containing the number of samples obtained from CLFM measurements and their respective results of the precision level. Based on a disjunctive table, the MCA plot was used to visualize the relationships between three or more categorical variables. The multiple regression analysis was also conducted in excel by using CLFM precision values as dependent response, while the environmental conditions for pH, temperature, salinity, and particles as independent predictor. This analysis aims to find the significant contributors among various environmental condition, and then predict the precision values for the further analysis.

Results and Discussion

1. Influence of salinity on CLFM measurement

As reported by Emam et al., produced water varies considerably depending on the geographic locations of the oilfield reservoirs, the geochemistry, types of hydrocarbons produced, and the types of the producing wells.[25] Therefore, this study investigated two types of oil samples, one with low API (higher density) and another with high API (low density) to take into consideration different oil types. In produced water, salinity varies tremendously, and many researchers have indicated that oil-in-water stability, as well as the produced water property, will be affected greatly by the presence of salts.[9, 26] In order to determine the CLFM measurement accuracy and precision under different salt concentrations, synthetic produced water samples with NaCl concentrations ranging from 35,000 to 250,000 ppm were used. The rationale for the selection of this salinity range was because produced water effluents can have salinity levels higher than the seawater (35,000 ppm) and occasionally can reach close to 250,000 ppm.[6]

The results of synthetic produced water under different salinities with the heavy and light oil samples were presented in Figure 1. The comparison of the CLFM analysis under each salinity was done using box-whisker plots. In this study, we used the mean/SE/SD mode, where SE stands for the standard error (standard deviation of the mean), and SD represents standard deviation of the dataset.[27] As can be seen in all plots, the dot in each plot represents the mean value of nine CLFM measurements, while the central line inside the box is the median value. The edges of the large box are calculated through mean ± SE, and the whiskers are derived from mean ± SD.[27] This analysis allowed us to determine any trends in the CLFM data distribution due to changes in various salinities. The accuracy and precision under different salinity were also calculated and shown in Table 1.

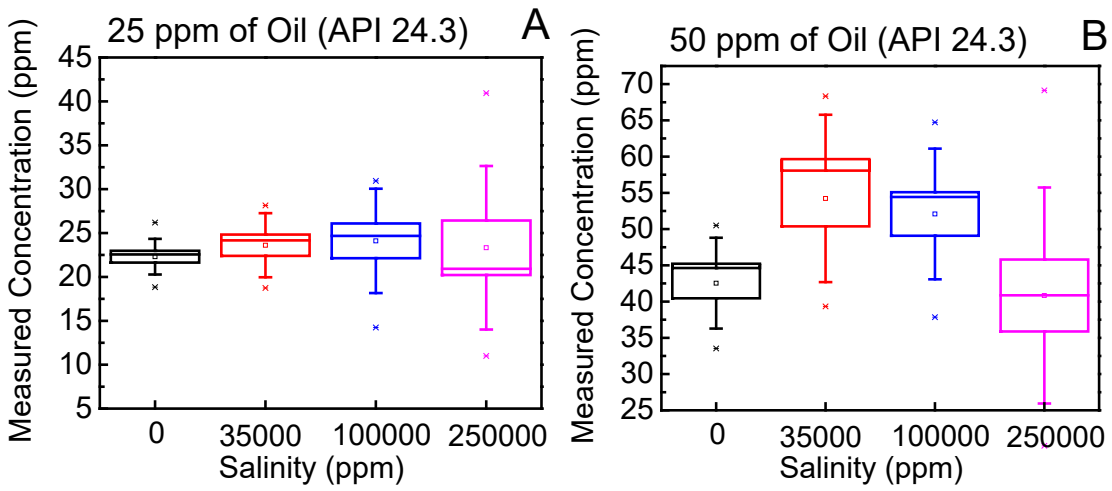

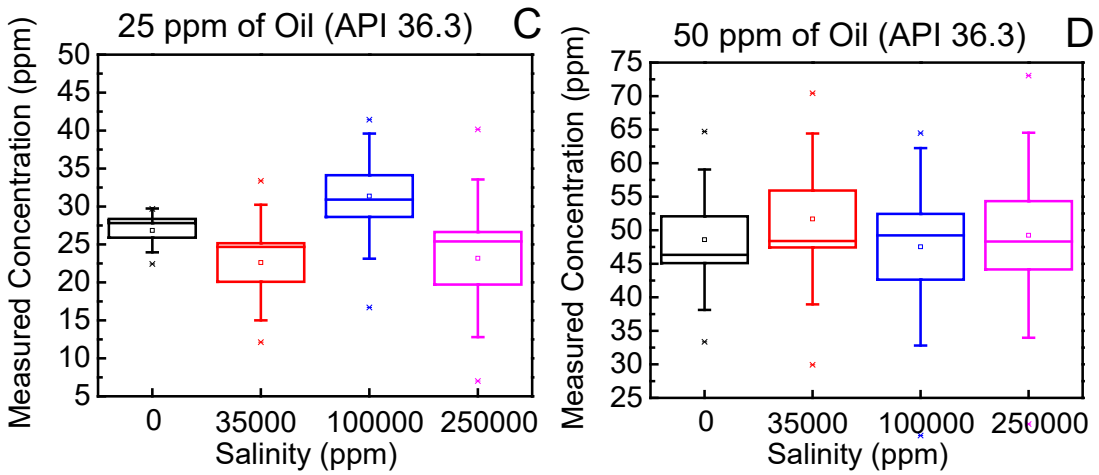

Figure 1. CLFM measurements for produced water prepared with crude oils with different API values (API 24.3 – heavy oil and API 36.3 -light oil). The dot inside the box represents the mean value, and the line inside the box represents the median value in the dataset. The box is plotted by mean ± standard error, and the whisker is plotted by mean ±standard deviation. The dots outside the boxes and whiskers are data beyond the range of mean ± standard deviation.

Table 1. Quantification of oil content in synthetic produced water samples using the CLFM method under different salinity. Synthetic produced water was prepared with 25 and 50 ppm of oil content.

	Salinity (ppm)		**0**	**35000**	**100000**	**250000**
Oil API 24.3	**25 ppm**	**Accuracy**	89.2%	94.4%	96.4%	93.3%
		Precision	8.1%	14.6%	23.8%	37.3%
	50 ppm	**Accuracy**	85.1%	108.4%	104.2%	81.7%
		Precision	12.5%	23.1%	18.0%	29.8%
Oil API 36.3	**25 ppm**	**Accuracy**	107.4%	90.5%	125.5%	92.7%
		Precision	11.5%	30.5%	33.0%	41.5%
	50 ppm	**Accuracy**	97.2%	103.4%	95.1%	98.5%
		Precision	20.9%	25.5%	26.4%	30.6%

As shown in Figure 1, large box-whiskers were typically observed for 250,000 ppm of salt, which suggested more scattered dataset. For samples with little or zero salinity, narrower box-whiskers were observed. This result shows that salinity affects the standard deviation of CLFM measurements. This observation is confirmed by the CLFM measurement precision in Table 1, which indicated that the precision of CLFM for synthetic produced water at salinity of 250000 ppm is 31% to 78% higher than the measurements for the synthetic produced water without salts. On the other hand, the accuracy for majority of the CLFM measurements under salinity range from zero to 250000 ppm fall into the EPA acceptable recovery range, which is 78% to 114%.[24]

Also, the oil droplet size histograms under different salinities were investigated to evaluate the salts impact on size distribution. As shown in Figure 2(a), 26 times more oil droplets in smaller size (around 4 μm) were observed for synthetic produced water without salts as compared to synthetic produced water with salinity of 250000 ppm. In contrast, the synthetic produced water with 250000 ppm of salinity had 5.1 times more oil droplets with larger sizes (>9 μm) comparing with 0 ppm of salinity. Similar trends were observed for 25 ppm of synthetic produced water prepared with oil at API 36.3 as shown in Figure 2(b). The 50 ppm samples of synthetic produced water prepared with API 24.3 and API 36.3 also showed similar results (Figure S1). A similar observation was also reported from the study of Moradi at al, who investigated the average droplet size distributions under different salinities.[9] They observed an increase in number of larger droplets and decrease in the frequency of smaller droplets in oil emulsions with 10% salinity as opposed to emulsions with 1% salinity.[9]

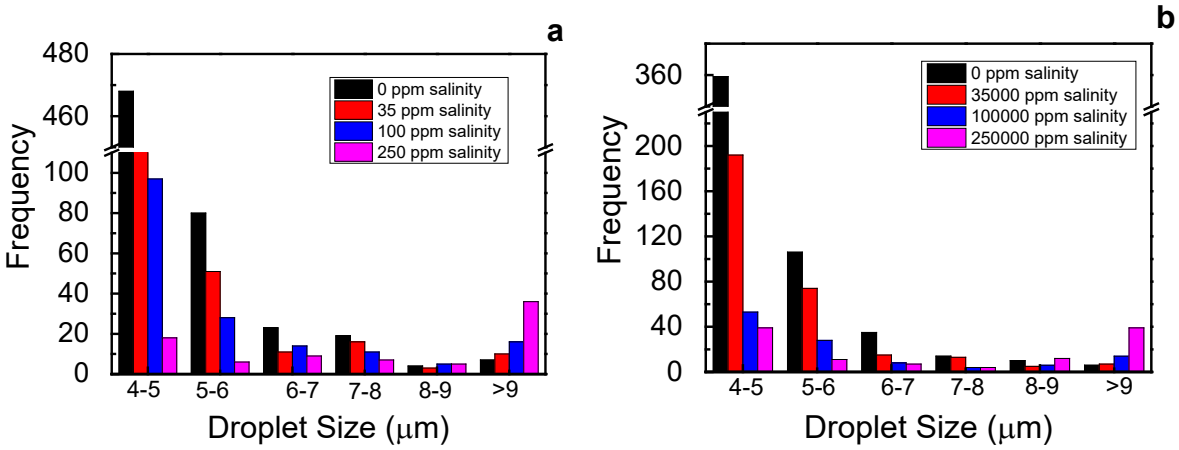

Figure 2. Oil droplet size histogram (a) 25 ppm of synthetic produced water prepared by oil with API 24.3 under salinity of 0, 35000, 100000 and 250000 ppm; (b) 25 ppm of synthetic produced water prepared by oil with API 36.3 under salinity of 0, 35000, 100000 and 250000 ppm.

It has been reported that the dominant destabilization mechaism for oil-in-water emulsion containing hydrocarbons is Ostwald ripening.[28-30] Therefore, the Ostwald ripening process was investigated in this study. The Ostwald ripening process is generally modeled by the Lifshitz-Slyozov-Wagner (LSW) theory for oil in water emulsions without excess of surfactant. The Ostwald ripening rate ω_t can be determined in Equation 8 as following:

$$\omega_t = \frac{8\gamma C_w^{eq} D_w V_m}{9K_B T} \quad (8)$$

where γ is the interfacial tension between oil and aqueous phase, V_m is the molecular volume of the oil, C_w^{eq} is the aqueous oil solubility, D_w is the diffusivity of the oil molecule, K_B is the Boltzmann constant and T is the absolute temperature. In order to understand the Ostwald ripening process, the interfacial tension was measured and reported in Figure 3. In this study, the interfacial tension values for oil at API 36.3 with nanopure water in zero, 35,000 ppm, 100,000 ppm and 250,000 ppm of salt concentrations were 21 dynes/cm, 24 dynes/cm, 28 dynes/cm, and 34 dynes/cm, respectively. However, due to the dark color of the oil with API 24.3, the interfacial tension could not be precisely measured with the tensiometer. Hence, surface tensions of produced water prepared with API 24.3

and API 36.3 were also measured as the indicator for interfacial tension and the results were shown in supporting information (Figure S2). The results of surface tensions for synthetic produced water samples under different salinities revealed that higher surface tension was achieved at the highest salinity (250,000 ppm). This trend was consistent with the two types of oils under various salt and oil concentrations. Through the surface tension measurements of oil with API 24.3, it is reasonable to hypothesize that the interfacial tension also increased with salinity for oil with API 24.3. Same trend of interfacial tension changes for water/pure hydrocarbon system were reported in other studies.[31, 32]

The change on the interfacial tension of oil and water after adding NaCl can be explained by the Gibbs adsorption isotherm, which relates the change in interfacial tension of a solution to the change in surface excess concentration of the components in the solution (Equation 9)

$$d\gamma = -RT\sum \tau_d \, lnC \tag{9}$$

where $d\gamma$ is the change in interfacial tension, R presents the universal gas constant, T denotes the absolute temperature, τ_d is the surface excess concentration, and C exhibits the bulk concentration of surface-active species.[31] The surface active components in the system include both salts in the water and surface-active agents in the oil. It has been provided that NaCl concentration are depleted at the water-vapor interface and the surface excess concentration of salts is negative through both experimental measurement and theoretical simulation ($\tau_{salts} < 0$).[33] Therefore, the change of interfacial tension will be positive due to the depletion of salts on the aqueous side of the oil-water interface.

For the surface excess concentration of crude oil components, due to the complexity of oil properties and composition, their effect towards interfacial tension still remain opaque. Moeini et al. mentioned that resins, waxes, and asphaltenes might work as surfactants and then adsorb at the oil-

water interface to increase the surface excess concentration and lower the interfacial tension. However, it has been reported that when salt concentration is higher than 40,000 ppm, the salt depletion effect in the aqueous phase will dominate and result in the large increase in the interfacial tension.[31] This is consistence with the observation in this study. However, further studies are needed to fully understand the interaction between surface-active reagents in the oil with salts and their influence on the interfacial tension.

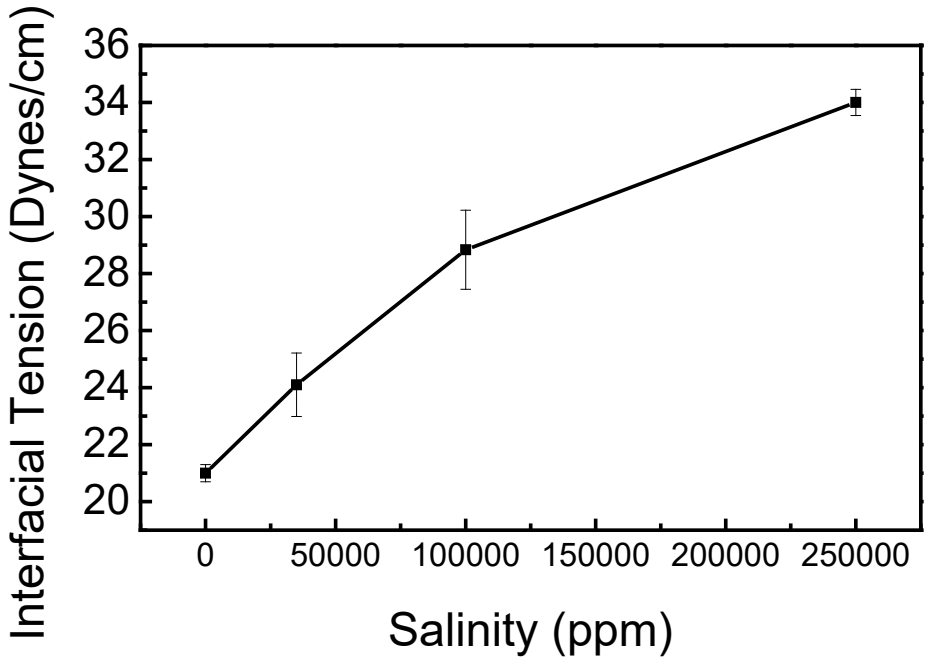

Figure 3. Interfacial tension between saline water at zero, 35000, 100000, and 250000 ppm of salt concentration and oil with API 36.3.

Aqueous oil solubility is another important factor to conduct the Ostwald ripening rate calculation (Equation 9). It is well known that increased salt concentration will reduce the oil solubility. Hence, the ratio of increase on interfacial tension and the ratio of decease on solubility would work together to determine the change of Ostwald ripening under different salinity. However,

due to the complexity of oil composition, there is lack of a comprehensive analytical method to accurately quantify all the hydrocarbons' solubility in crude oil.[34]

From the thermodynamic point of view, the driving force for Ostwald ripening is the difference of Laplace pressure between droplets.[35] Hence, Laplace pressure was calculated in this study to prove the Ostwald ripening process. Laplace pressure is the pressure difference between the inside and the outside of a droplet and it defined by the Young-Laplace equation (Equation 10)

$$\Delta P = \frac{2\sigma}{R} \tag{10}$$

where σ is oil/water interfacial tension, and R represents radius of the droplet. The Laplace pressure for 25 ppm of oil with API 36.3 was calculated and presented in Table 3. However, due to the lack of interfacial tension values for oil with API 24.3 under various salinity, Laplace pressure was only calculated for oil with API 36.3. As shown in table 2, a 35% higher Laplace pressure was observed for synthetic produced water (prepared by oil with API 36.3) with 250,000 ppm of salt concentration as compared to the synthetic produced water without salt. It has been reported that droplet stability increase due to the decrease in the Laplace pressure.[36] In our study, higher Laplace pressure caused by high concentration of salts would result faster Oswtald ripening process, which in turn show a less precise measurement with the CLFM.

Table 3. Initial average droplet size after mixing, interfacial tension and Laplace pressure for 25 ppm of synthetic produced water prepared with oil at API 36.3 in different salinity

Salinity	Average Droplet Size (um)	Interfacial Tension (Dynes/cm)	Laplace Pressure (KPa)
0 ppm	4.84	21	8.67
35,000 ppm	4.88	24	9.83
100,000 ppm	5.16	28	10.85

250,000 ppm	4.75	34	14.31

Polydispersity index affects the Ostwald ripening significantly as higher polydispersity will lead to a faster Ostwald ripening rate.[37] In this study, the polydispersity index was calculated according to the previous reported method.[38] The Spearman rank correlation coefficient of 0.87 between initial polydispersity index with average oil droplet size (Figure 4(a)) showed that the oil-water emulsion with higher initial polydispersity under higher salinity will lead to faster Ostwald ripening process, and result in the bigger average oil droplets size during the analysis. Hence, the Oswald ripening process which alters the oil droplet stability will decrease the precision during the image acquisition of CLFM measurement as shown in Figure 4 (b). Furthermore, the ionic strength in the oil-water emulsion could also affects the repulsive barrier between the two droplets. It has been reported that increase in the ionic strength of the continuous phase significantly reduces the Debye screening length and hence lower the repulsive barrier.[39] Therefore, the oil-water emulsion having higher salinity will have a higher probability of aggregation. In conclusion, the increased interfacial tension for oil-water interface under higher salinity could increase the Laplace pressure, facilitating the Ostwald ripening process, and then reduce the detection precision of CLFM measurement.

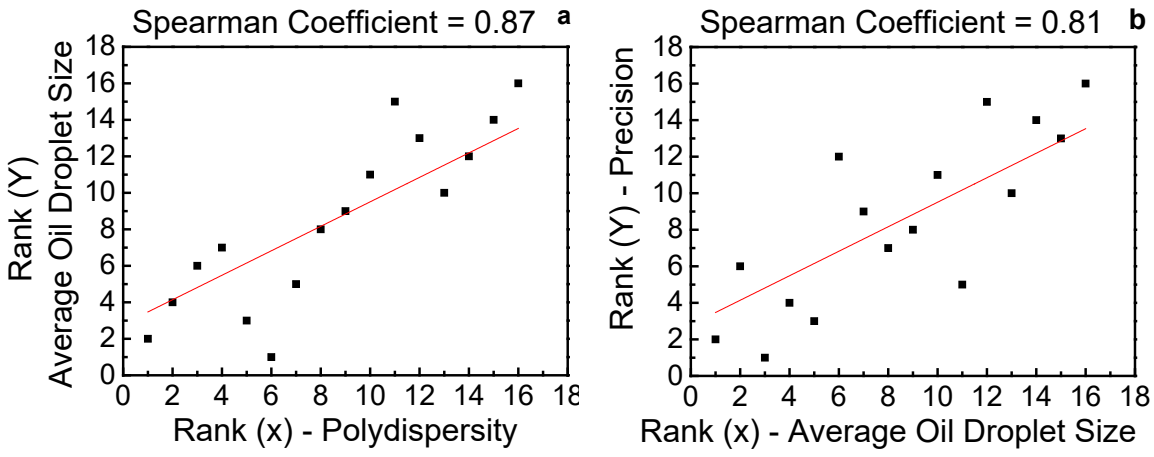

Figure 4: Spearman rank coefficient plots (a) Oil droplets polydispersity with average oil droplet size (b) average oil droplet size with CLFM precision for various produce water samples with zero, 35000, 100000, and 250000 ppm of salt concentration.

2. The effect of pH on CLFM measurement

The pH of produced water varies depending on the pressure of drilling mud and chemicals used during extraction.[40] Eman et al. also indicated that years of production and oilfield depths also affected the pH values of produced water.[25] As reported, the allowable pH values for seawater discharges were in the range of 7 to 8. However, studies investigating produced water pH ranges over a period of nine years found out that water samples discharged from oil platforms had values varying from 4.2 to 6.8, while produced water samples from gas platforms were between 3.5 and 5.[25, 41] Therefore, in this study, synthetic produced water samples were prepared with pH values varying from 3 to 8 to investigate their effects on CLFM measurements.

The results of CLFM measurements under different pH values of synthetic produced water were presented in Figure 5. Results showed larger box-whiskers for basic conditions, while the data are less scattered in acidic and neutral conditions. The narrower box-whisker was shown at pH 7, and this trend is similar for the two types of synthetic produced water investigated in this study.

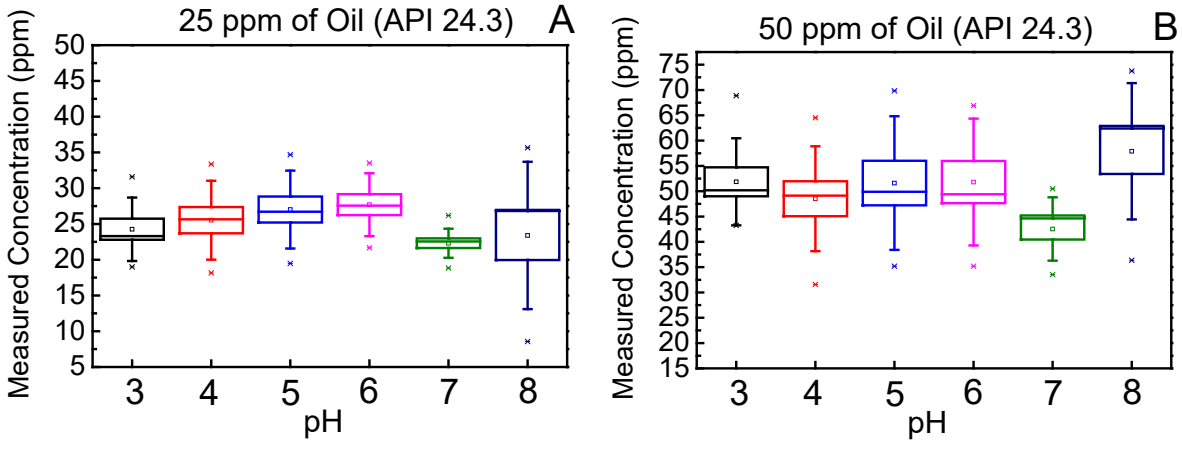

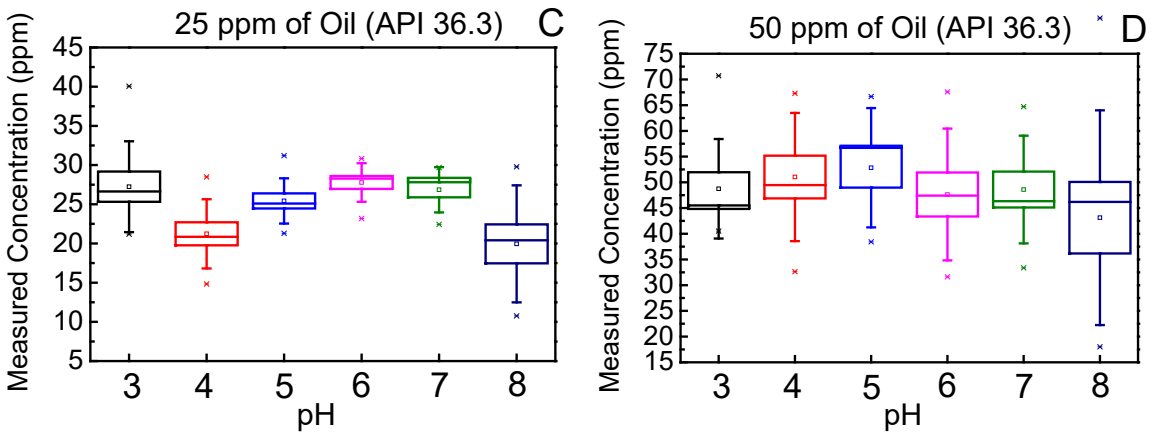

Figure 5. CLFM measurements for produced water prepared with crude oils with different API values under various pH. The dot inside the box represents the mean value, and the line inside the box represents the median value in the dataset. The box is plotted by mean ± standard error, and the whisker is plotted by mean ±standard deviation.

The quantities determined by the CLFM measurement for accuracy and precision were shown in Table 4. As can be seen in Table 4, the majority of the CLFM measurements' accuracy under pH range between 3 and 8 fall into the EPA acceptable recovery range, which is 78% to 114%. However, the precision of CLFM measurement is 0.45 to 3.8 times higher than the EPA acceptable precision value (11%).[24] As discussed in our previous investigation, the small amount of sample volume for CLFM measurement, physical-chemical properties of the oil sample, microscope settings and sample preparation procedures might, together, contribute to cause the larger errors for CLFM measurements.[7] Furthermore, the precision under pH 8 is 7% to 63% higher than the acidic and neutral pH. These results indicated that pH might also influence the precision of CLFM measurements.

Table 4. Quantification of oil content in synthetic produced water samples using the CLFM method under different pH. Synthetic produced water was prepared with 25 and 50 ppm of oil content.

	PH		**3**	**4**	**5**	**6**	**7**	**8**
Oil API 24.3	**25 ppm**	**Accuracy**	97.1%	102.1%	108.1%	110.8%	89.2%	93.6%

		Precision	17.7%	22.1%	21.8%	17.6%	8.1%	41.2%
	50 ppm	**Accuracy**	103.7%	97.0%	103.2%	103.6%	85.1%	115.8%
		Precision	17.2%	20.7%	26.4%	25.1%	12.5%	26.9%
Oil API 36.3	**25 ppm**	**Accuracy**	109.0%	84.9%	101.7%	111.1%	107.4%	77.8%
		Precision	23.2%	17.6%	11.5%	9.8%	11.5%	29.9%
	50 ppm	**Accuracy**	97.5%	102.1%	105.7%	95.3%	97.2%	86.2%
		Precision	19.3%	24.9%	23.2%	25.6%	20.9%	41.8%

Like for salinity, various studies have also reported that interfacial tension correlates with pH.[42] However, no statistically significant changes were observed on interfacial tensions under these pH values in this study (Figure S3, S4). The same trend was also observed on some crude oil samples.[43] Therefore, the interfacial tension might not explain the observed phenomen in this study when low concentrations of surface active components are present in the water sample.

It has been demonstrated that collision effects, van der Val's forces, capillary forces and electrostatic effects can contribute to the interaction between oil droplets, and lead to changes in oil droplet stability.[44] Therefore, the interactions including attraction and repulsion between oil droplets under different pH were calculated and DLVO interaction energy plot was drawn to understand the energy interaction for oil droplets under different pH.

The interaction energy profiles for 25 ppm of synthetic produced water at different pH prepared by oil with API 24.3 and 36.3 were shown in Figure 6. In general, all the figures are mostly overlap, indicating that the samples under different pH showed similar energy barrier. On the other hand, the zoom in the figure demonstrated that secondary minima were formed in the interaction energy profiles

at these three pH values. The deepest secondary minimum was found at pH 8, while shallower peaks were shown at pH 3 and pH 7. Similar trend was also observed in Figure 6 (b) which is synthetic produced water prepared with the oil of API 36.3. It has been reported that droplets may undergo a reversible flocculation due to the secondary minimum because of its weak energy barrier, resulting in slow droplets aggregation.[45] Hence, a deeper secondary minimum at pH 8 might result in a faster aggregation and consequently lead to a more unstable colloidal system. Similar observations are reported in by other studies.[46] In conclusion, deeper secondary minima for the synthetic produced water at pH 8 might go through reversible flocculation, which affect the CLFM measurement precision. However, it is hard to conclude that pH will have a great effect on the interactions of oil droplets under different pH based on the overlapped DLVO plot.

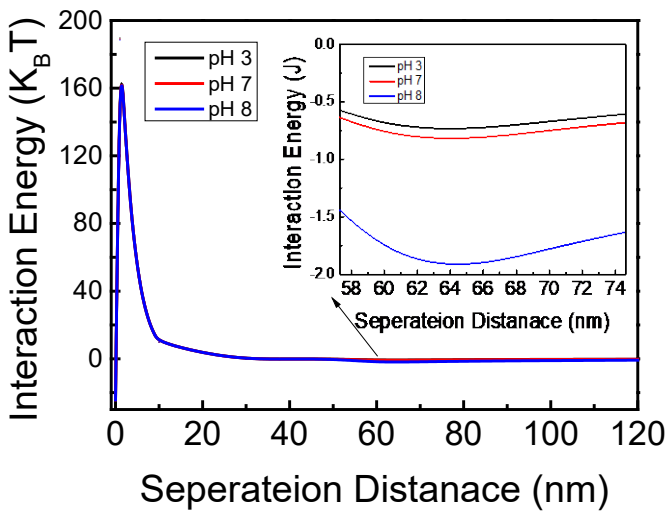

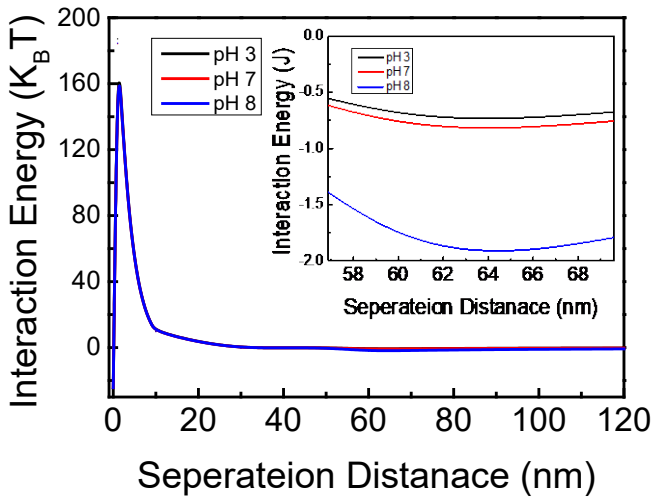

Figure 6. DLVO interaction for synthetic produced water under various pH (a) Interaction energy of oil droplets in 25 ppm of synthetic produced water prepared by oil at API 24.3. (b) Interaction energy of oil droplets in 25 ppm of synthetic produced water prepared by oil at API 36.3.

3. Temperature effects on CLFM measurement

Previous studies have shown that the temperature of produced water will change with different treatment types and locations. For example, Erdlac et al. reported that Texas has thousands of oil and gas wells that can reach temperatures over 100 ºC.[47, 48] On the other hand, produced water samples in arctic environments have low temperatures.[13] Hence, the temperature of produced water should also be considered as a parameter that could affect CLFM measurements. In this study, three temperature values (4 ºC, 25 ºC, and 60 ºC) were investigated to test their influence on accuracy and precision of CLFM measurements.

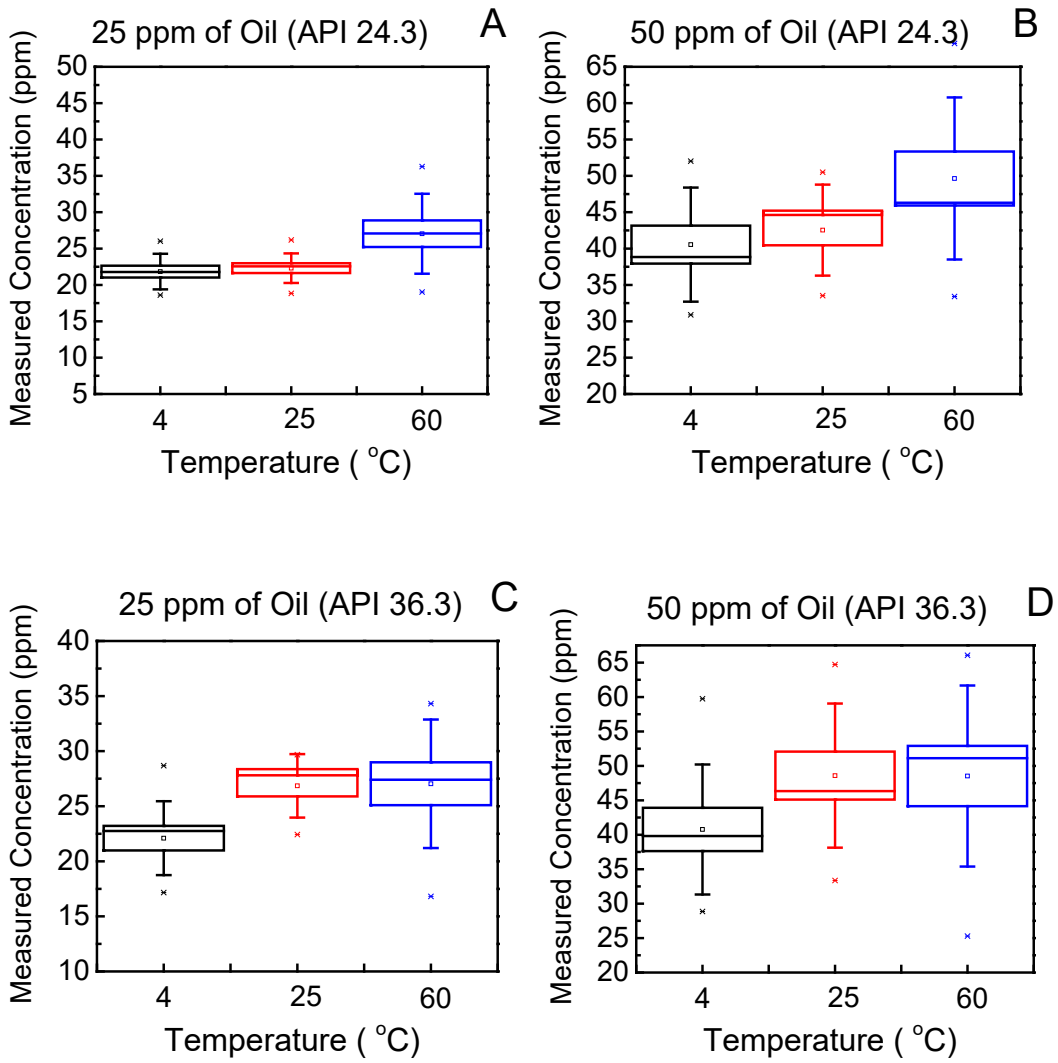

Figure 7. CLFM measurements for produced water prepared with crude oils with different API values under different temperature. The dot inside the box represents the mean value, and the line inside the box represents the median value in the dataset. The box is plotted by mean ± standard error, and the whisker is plotted by mean ±standard deviation.

As shown in Figure 7, the average CLFM detection values at 4 ºC were 4.3 % to 17.8 % smaller than the concentrations detected at higher temperatures. This trend is consistent with the CLFM accuracy calculation. The lower detection concentration at 4ºC could be attributed to changes in solubility of hydrocarbons in water under different temperature. It has been reported that elevated temperature could increase the diffusion coefficient, leading to a more soluble hydrocarbon. Thus, a

higher average value was observed under 60 ºC temperature due to larger amounts of dissolved organic hydrocarbons.

Furthermore, more concentrated data were observed in box-whisker plots at 4 ºC and 25 ºC, while larger box-whiskers were shown for the samples at 60 ºC. The precision of CLFM measurement in Table 6 also confirmed that 1.2 to 2.3 times less precise measurements were observed under 60 ºC. This indicated that CLFM measurements are more precise at room temperatures or lower. It has been reported that temperature can affect emulsion stability.[1] Our results confirmed that the synthetic produced water and oil/water emulsion properties change with increasing temperatures. The increase in temperature will increase the kinetic energy of the oil droplets and decrease the viscosity of liquid, which will lead to increased velocity of coalescence and separation according to the Stokes' equation.[49] It was also widely validated that collisions between particles will increase at higher temperatures.[50] As a result, the droplets will move faster and collide more frequently.[51] Therefore, in this study, the Brownian motion and collisions might be the reason for unstable oil droplets under high temperatures.

Table 6. Quantification of oil content in synthetic produced water samples using the CLFM method under different temperature. Synthetic produced water was prepared with 25 and 50 ppm of oil content.

Temperature (ºC)			**4**	**25**	**60**
Oil API 24.3	**25 ppm**	**Accuracy**	87.4%	89.2%	108.2%
		Precision	9.8%	8.1%	22.0%
	50 ppm	**Accuracy**	81.1%	85.1%	99.3%
		Precision	13.6%	12.5%	22.3%
Oil API 36.3	**25 ppm**	**Accuracy**	88.4%	107.4%	108.2%

		Precision	13.4	11.5	23.3
	50 ppm	**Accuracy**	81.5%	97.2%	97.1%
		Precision	18.9%	20.9%	26.3%

4. Particle concentration effects on the CLFM measurement

Besides the environmental factors we discussed above, solids present in produced water might also affect the CLFM measurement. It has been reported that produced water discharge after treatment process could reduce silica concentration below 50 ppm.[14] Hence, 25 and 50 ppm of silica (SiO_2) were selected to test if its presence in the synthetic produced water will affect CLFM accuracy and precision. The CLFM measurements are presented in Figure 9 and Table 7. As can be seen, by adding 25 ppm and 50 ppm of SiO_2, more than 147% increment of error were observed for crude oil with API 24.3. Similarly, the CLFM precision and accuracy also presented notable changes for 25 ppm and 50 ppm of synthetic produced water made with oil of API 36.3 after addition of 25 ppm SiO_2. Thus, the particles effects on CLFM measurements depend, not only, on the type and concentration of oil, but also on particle concentration in the system.

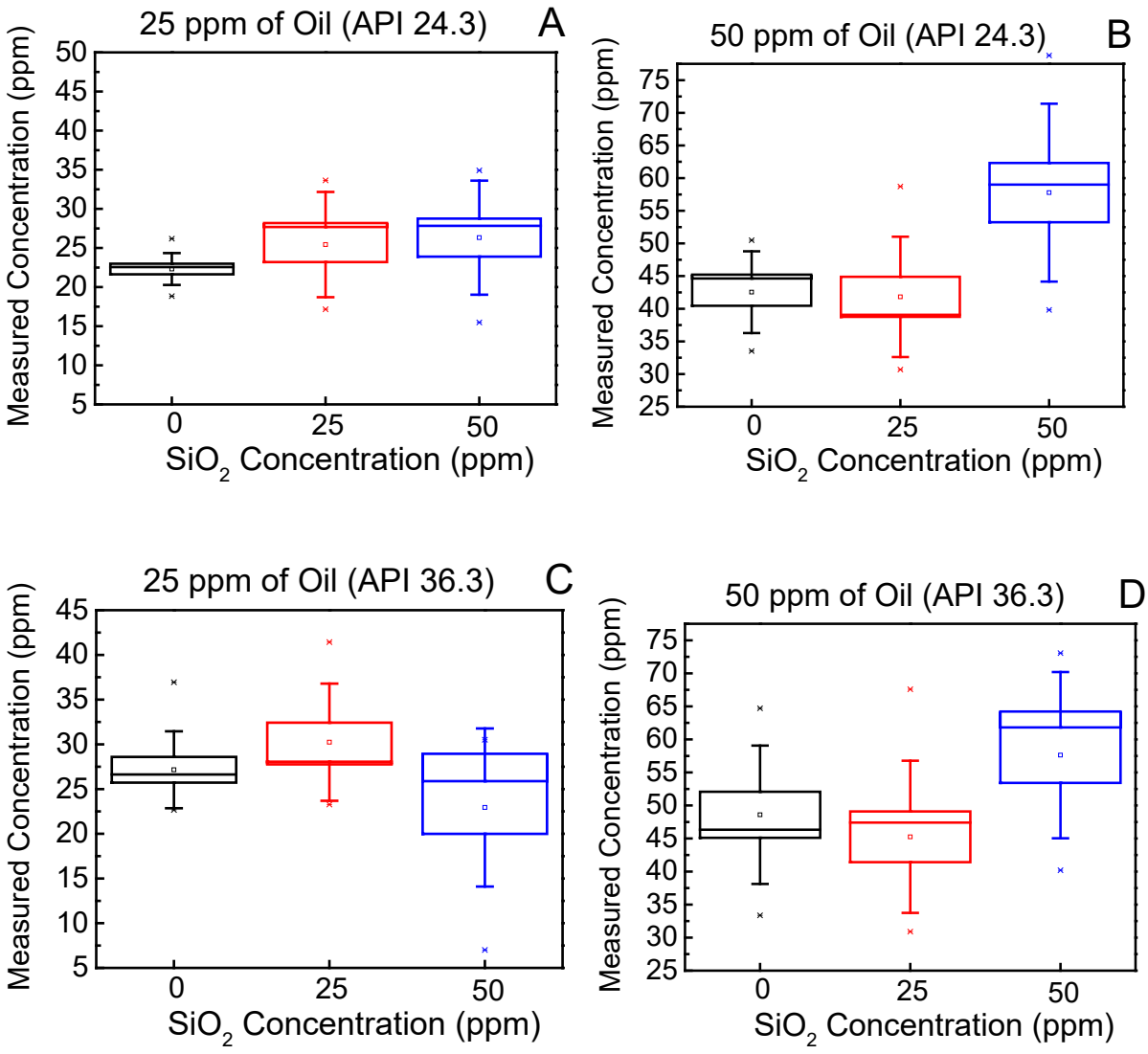

Figure 9. CLFM detection of different oil with SiO_2 particle. The dot inside the box represents the mean value, and the line inside the box represents the median value in the dataset. The box is plotted by mean ± standard error, and the whisker is plotted by mean ±standard deviation.

Table 7. Quantification of oil content in synthetic produced water samples using the CLFM method under different concentration of particles. Synthetic produced water was prepared with 25 and 50 ppm of oil content.

Particle Concentration (ppm)	**0**	**25**	**50**

Oil API 24.3	**25 ppm**	**Accuracy**	89.2%	101.8%	105.3%
		Precision	8.1%	26.9%	29.2%
	50 ppm	**Accuracy**	85.1%	83.6%	115.6%
		Precision	12.5%	18.4%	27.2%
Oil API 36.3	**25 ppm**	**Accuracy**	108.6%	121.0%	91.8%
		Precision	17.2%	26.2%	35.4%
	50 ppm	**Accuracy**	97.2%	90.5%	115.2%
		Precision	20.9%	23.0%	25.2%

In order to qualitatively understand the interactions between SiO_2 and oil droplets, DLVO theory was applied to assess and explain the oil and SiO_2 droplets aggregation. After calculation, the total energy for synthetic produced water under various conditions were presented in Figure 10.

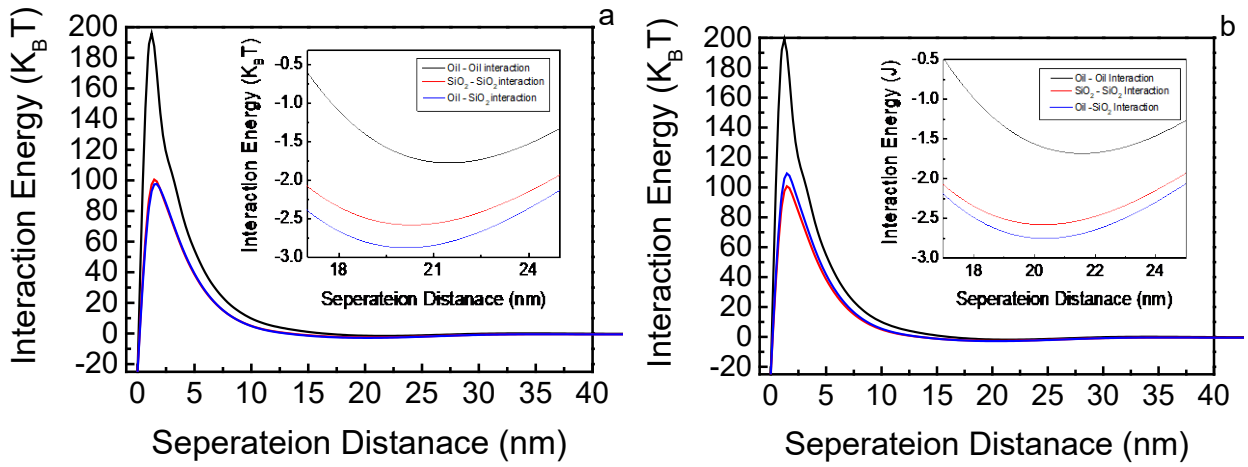

Figure 10. DLVO interaction energy between oil droplets, SiO_2 particles and oil with SiO_2 interaction (a) oil at API 24.3 (b) oil at API 36.3.

As can be seen in Figure 10 (a) and (b), the highest energy barriers for both figures were observed for oil droplets interaction which is 189 K_BT for oil with API 24.3 and 191 K_BT for oil with

API 36.3. These results confirmed that the samples contained only oil are more stable than the samples having particles interaction. In addition, higher concentration of oil are easier to pass the energy barrier and aggregate as shown in supporting information (Figure S7). Previous publication has proved that higher concentration of oil trend to have bigger coalescence rate, leading to a less precise CLFM measurement.[7] Therefore, oil droplets are considered as the most stable samples as shown in DLVO plot and the stability of oil droplets are related with oil concentration which higher oil concentration of oil droplets are less stable due to the faster coalescence rate.

Lower energy barrier was observed for SiO_2 particles and Oil and SiO_2 interaction in the synthetic produced water. The zoom in figure demonstrated that secondary minima were formed in the interaction energy profiles. This could link to the direct inter-particle bridging by acid-base bonds formed from silanol groups and dissociated SiO^- groups on oil-water mixture.[52] At pH 7, the acidic and basic groups in silica are coexisting on the particle surface, and then bound with each other to coagulate.[53] This observation is consistence with DLVO plot which showed in this study. Furthermore, it has been reported that resins and asphaltenes in the crude oil can be absorbed by silica surface, which might also facilitate the coagulation and precipitation process.[54] Hence, deepest secondary minima were observed for samples containing oil and SiO_2 particles.

Similar with salinity, the Spearman correlation coefficient was calculated to assess the relationship between average oil droplet size and CLFM measurement precision after adding particles in the system. The Spearman coefficient of 0.70 indicated that the increased average droplet size due to the coagulation and precipitation by adding SiO_2 has good correlation with increased CLFM precision value (decreased precision level) (Figure S8) . In conclusion, by adding SiO_2 in the synthetic produced water, the adsorption and bouding reaction between oil and SiO_2 could facilitate the coagulation of oil, leading to increased oil droplet size. When the oil droplets are unstable and

coagulate, the homogenization of sample decreased, which in turn decrease the precision level of CLFM measurement.

Relationship of environmental variables with CLFM precision

Since CLFM is sensitive to drastic oil droplet changes, understanding the environmental conditions that are more favorable for a more precise CLFM measurement is important to determine the suitability of the technique for different environmental conditions. To statistically understand the relationship of environmental variables with precision of the method, a multiple correspondence analysis (MCA) was conducted. MCA is a factor analysis approach which considers to be an extension of simple correspondence analysis to more than two variables.[55] MCA is used to produce a graphical representation of a set of categorical variables, based on all possible pairs of cross tabulations. MCA can project different variables onto a two-dimensional plane. The relationship between variables can be deduced from the relative positions of the modalities of the variables on the planes.[56] More than that, MCA possesses similar advantage to principal component analysis, but also more readily allows the recoding of categorical data for analysis.[57]

In this study, different environmental conditions like pH, temperature, salinity and concentration of particles are considered as categorical variables, while the level of precision from CLFM analysis coded into low, medium and high are the supplementary variables.

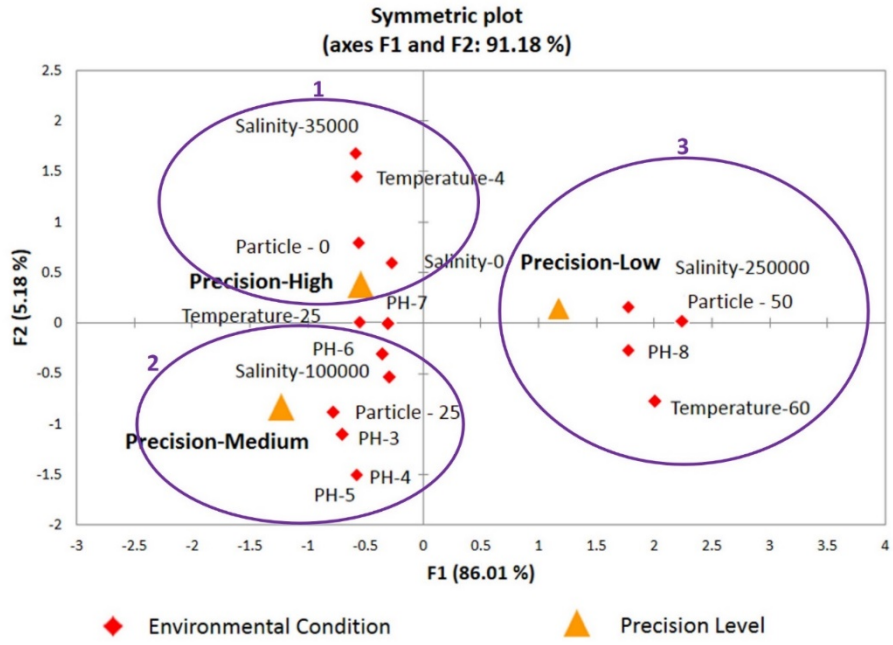

Figure 11. MCA analysis for CLFM detection measurement with different environmental parameters (pH, temperature, salinity and particle concentration. Precision High correspond to a precision value <20%, Precision - Medium correspond to a precision value between 20% and 40%, and Precision - High corresponds precision value > 40%.

Figure 11 shows the results of MCA regarding the relationship among the levels of CLFM precisions and environmental parameters on CLFM measurements. The origin on the map corresponds to the centroid of each variable. Therefore, the distance from an object to the origin is the reflection of the variation from the "average" pattern (the most frequent category for each variable). Objects with similar characteristics with average pattern lie near the origin, whereas objects with unique characteristics are located far from the origins. Therefore, in our study, the samples with pH 7 were is the most frequent properties among all the sample. Furthermore, there are two dimensions in the graph where dimension 1 is represented by the horizontal axis and dimension 2 as vertical axis are exhibit in Figure 11. The dimensions' label represents the visualization display of the variance in the data. In our study, 86.01% of variance is represented in dimension 1, while 5.18%

of the variance is represented by dimension 2. Therefore, MCA plot in this study represent total 91% of the variance. Along dimension 1, “Particle-50” is furthest away from the origin and therefore has the most importance. Along dimension 2, “Salinity-35000” has the most importance. These results indicated that the most important difference or largest deviation from independence in the sample is between the samples having condition as “Particle -50” and the other samples. The second most importance difference is between samples having conditions as “Salinity-35000” and other samples. The importance of data can also be viewed as the contribution of each variable for each dimension, which is listed in the contribution table as shown in supporting information. In this study, “Salinity-35000” and “Particle -50” has the highest contribution for dimension 1 and 2.

In addition, the closeness of points on the map with regards to their angle from the origin and points in the same quadrant can be used as guidelines to interpret relationships between variables. Three clusters can be isolated in accordance with the results of linear regression. In the top left quadrant, the “Precision - High” is associated with “salinity - 35,000 ppm”, “Temperature - 4 ^{o}C”, “Salinity – 0 ppm” and “Particle concentration - 0 ppm” and represented as a first cluster. A second cluster group with “pH - 3 to 6”, “Particle concentration - 25 ppm”, and “Salinity - 100,000 ppm” showed in the left bottom quadrant, corresponded to the “Precision-Medium.” In the right panel of the graph, a third cluster including “Salinity - 250,000 ppm”, “Temperature - 60 ^{o} C”, “Particle concentration - 50 ppm”, and “pH – 8” are pertain to “Precision-High” response. “pH – 7” and “Temperature – 25 ^{o}C” showed in the x-axis correlates better with the “Precision-High”. This analysis confirmed that synthetic produced water without particles, at medium pH, low salinity and room or even lower temperature is related to more precise CLFM measurement, while higher temperature, high concentration of particles and base pH would attribute to a less precise CLFM measurement.

This finding is in agreement with our previous observation and helps us to understand the optimum conditions for CLFM measurement.

Multivariate regression analyses were also another type of statistical analysis to estimate the relationships among various variables and then predict the value of response. In this study, the precision value is considered as the dependent values (response), and the condition of pH, temperature, salinity, and particle concentrations are independent variables (predictor). The results of multivariate regression analysis were shown in Table 8. The p-value in the regression model tests the null hypothesis that the coefficient of predictor has no effect to the depended response. A low p-value (< 0.05) indicates that the null hypothesis is rejected. In other words, a predictor that has a low p-value is likely to be a meaningful addition to the model, since the changes in the predictors' value are related to the changes in the response variable. In this study, pH and temperature have high p-values which are 0.58 and 0.71 respectively, which indicate that they are not statistically significant. However, salinity and particles showed significant contribution to the response in this study by small p-values which are 0.00885 and 0.00762, respectively. This could also be confirmed by the MCA analysis which indicate that "Particle -50" and "Salinity-35000", which have the major contribution to the dimensions. The Spearman correlation coefficient for CLFM precision with salinity, pH, temperature, and particles also confirmed that particle and salinity have higher correlation coefficient as compared with pH and temperature as shown in the supporting information.

Table 8. Multivariate regression analysis for precision value as the response, pH, temperature, salinity and particle concentration as predictors.

	Coefficients	Standard Error	t Stat	P-value	Lower 95%	Upper 95%
Intercept	20.193	5.399	3.740	0.000	9.360	31.027
PH	0.435	0.791	0.551	0.584	-1.151	2.022
Temperature	-0.027	0.074	-0.362	0.719	-0.176	0.122

Salinity	0.000	0.000	2.720	0.009	0.000	0.000
Particle Concentration	0.199	0.072	2.776	0.008	0.055	0.343

Finally, through re-running the multivariate regression analysis with excluding insignificant factors (pH and temperature), the equation 11 was generated and might help to predict the precision level for future analysis with R^2 as 38%. The predicted precision values generated from multivariate regression model and the observed precision values were compared and shown in Figure 12 with 95% confidence interval. As can be seen in Figure 12, even the R is 38%, the model has a relatively good prediction as compared with observed value. However, thorough understanding of how environmental parameter will affect the oil droplets stability are necessary in order to have a more precise model to predict the CLFM precision level.

$$Y = 22.31 + 3.57 \times 10^{-5} X_1 + 0.19 X_2 \quad (11)$$

where Y is the CLFM measurement precision, X_1 represent salt concentration, and X_2 is the particle concentration

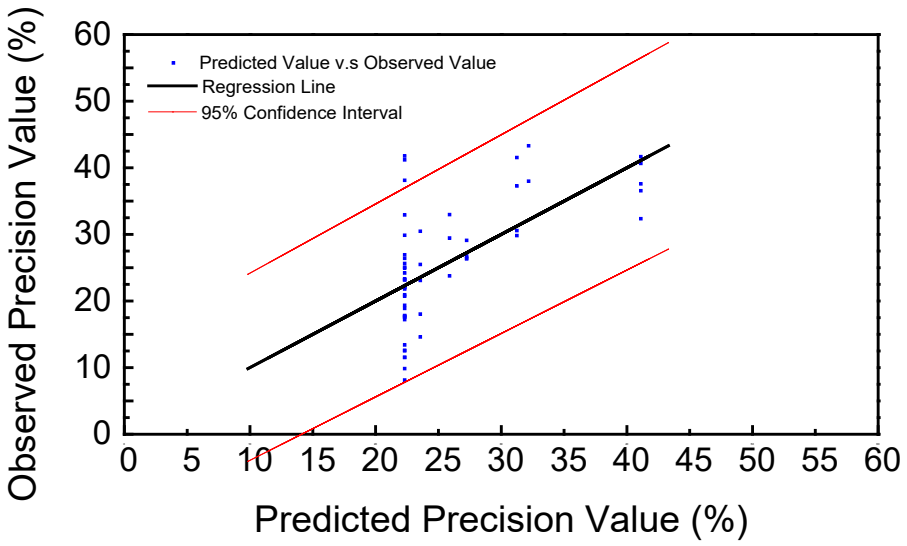

Figure 12. The relationship between predicted CLFM precision values calculated from multivariate regression analysis with observed precision value under different environmental parameters.

Conclusion

The CLFM method was able to accurately quantify oil concentrations in different types of synthetic produced water. However, the environment parameters including pH, salinity, temperature and particle concentrations will affect the precision of CLFM measurement at different levels due to the stability of oil droplet emulsion through Ostwald ripening, flocculation, and Brown motion. Hence, further studies to minimize the standard deviation and to improve the method precision is important to make CLFM measurements more applicable in real field and comparable to the EPA method. Furthermore, the precision of CLFM detection might be improved by adjusting the water sample into the optimum condition of CLFM measurements that would lead to higher precision of the analysis.

Acknowledgements

Funding for the project (Project No. 12121-6301-03) was provided through the "Ultra-Deepwater and Unconventional Natural Gas and Other Petroleum Resources Research and Development Program" authorized by the Energy Policy Act of 2005. This program—funded from lease bonuses and royalties paid by industry to produce oil and gas on federal lands—is designed to assess and mitigate risk enhancing the environmental sustainability of oil and gas exploration and production activities. RPSEA is under contract with the U.S. Department of Energy's National Energy Technology Laboratory to administer three areas of research. We also would like to acknowledge the National Science Foundation Career Award #: 1150255 for partially supporting the student Jingjing Fan.

Reference

1. Bakke, T.; Klungsøyr, J.; Sanni, S., Environmental impacts of produced water and drilling waste discharges from the Norwegian offshore petroleum industry. *Marine Environmental Research* **2013,** 92, 154-169.
2. Veil, J., US produced water volumes and management practices in 2012. *Report prepared for the ground water protection council* **2015**.
3. Patin, S. A.; Cascio, E., *Environmental impact of the offshore oil and gas industry*. JSTOR: 1999; Vol. 1.
4. Stephenson, M., A survey of produced water studies. In *Produced water*, Springer: 1992; pp 1-11.
5. Veil, J. A.; Puder, M. G.; Elcock, D.; Redweik Jr, R. J., A white paper describing produced water from production of crude oil, natural gas, and coal bed methane. *Argonne National Laboratory, Technical Report* **2004**.
6. Fakhru'l-Razi, A.; Pendashteh, A.; Abdullah, L. C.; Biak, D. R. A.; Madaeni, S. S.; Abidin, Z. Z., Review of technologies for oil and gas produced water treatment. *Journal of hazardous materials* **2009,** 170, (2), 530-551.
7. Fan, J.; Sappington, E. N.; Rifai, H. S.; Rodrigues, D. F., Confocal microscopy as a new real-time quantification method for oil content in produced water. *Journal of Petroleum Science and Engineering* **2018**.
8. Khelifa, A.; Stoffyn-Egli, P.; Hill, P. S.; Lee, K., Effects of salinity and clay type on oil–mineral aggregation. *Marine environmental research* **2005,** 59, (3), 235-254.
9. Moradi, M.; Alvarado, V.; Huzurbazar, S., Effect of salinity on water-in-crude oil emulsion: evaluation through drop-size distribution proxy. *Energy & fuels* **2010,** 25, (1), 260-268.
10. Alvarado, V.; Wang, X.; Moradi, M., Stability proxies for water-in-oil emulsions and implications in aqueous-based enhanced oil recovery. *Energies* **2011,** 4, (7), 1058-1086.
11. Souza, W.; Santos, K.; Cruz, A.; Franceschi, E.; Dariva, C.; Santos, A.; Santana, C., Effect of water content, temperature and average droplet size on the settling velocity of water-in-oil emulsions. *Brazilian Journal of Chemical Engineering* **2015,** 32, (2), 455-464.
12. Lambert, R. A.; Variano, E. A., Collision of oil droplets with marine aggregates: Effect of droplet size. *Journal of Geophysical Research: Oceans* **2016,** 121, (5), 3250-3260.
13. Zheng, J.; Chen, B.; Thanyamanta, W.; Hawboldt, K.; Zhang, B.; Liu, B., Offshore produced water management: A review of current practice and challenges in harsh/Arctic environments. *Marine pollution bulletin* **2016,** 104, (1), 7-19.
14. Ray, J. P.; Engelhardt, F. R., *Produced water: Technological/environmental issues and solutions*. Springer Science & Business Media: 2012; Vol. 46.
15. Hagstrom, R. A.; Finch, S. R.; Lynn, T. D., Apparatus for quantitative determination of total base or acid number of oil. In Google Patents: 1998.
16. Cortés-Estrada, A.; Ibarra-Bracamontes, L.; Aguilar-Corona, A.; Viramontes-Gamboa, G.; Carbajal-De la Torre, G., Surface tension and interfacial tension measurements in water-surfactant-oil systems using pendant drop technique. In *Experimental and Computational Fluid Mechanics*, Springer: 2014; pp 219-226.
17. Harendra, S.; Vipulanandan, C., Effects of surfactants on solubilization of perchloroethylene (PCE) and trichloroethylene (TCE). *Industrial & Engineering Chemistry Research* **2011,** 50, (9), 5831-5837.
18. Kakizawa, Y.; Harada, A.; Kataoka, K., Environment-sensitive stabilization of core− shell structured polyion complex micelle by reversible cross-linking of the core through disulfide bond. *Journal of the American Chemical Society* **1999,** 121, (48), 11247-11248.

19. Pashley, R., DLVO and hydration forces between mica surfaces in Li+, Na+, K+, and Cs+ electrolyte solutions: A correlation of double-layer and hydration forces with surface cation exchange properties. *Journal of Colloid and Interface Science* **1981,** 83, (2), 531-546.
20. Gregory, J., Approximate expressions for retarded van der Waals interaction. *Journal of Colloid and Interface Science* **1981,** 83, (1), 138-145.
21. Valmacco, V.; Elzbieciak-Wodka, M.; Besnard, C.; Maroni, P.; Trefalt, G.; Borkovec, M., Dispersion forces acting between silica particles across water: influence of nanoscale roughness. *Nanoscale Horizons* **2016,** 1, (4), 325-330.
22. Everett, D. H., *Basic principles of colloid science*. Royal society of chemistry: 1988.
23. Silva, F.; Tavares, F.; Cardoso, M., Thermodynamic stability of water-in-oil emulsions. *Brazilian Journal of Petroleum and Gas* **2013,** 7, (1).
24. USEPA, E., Method 1664 revision A: N-hexane extractable material (HEM; oil and grease) and silica gel treated N-hexane extractable material (SGT-HEM; non-polar material) by extraction and gravimetry. *Washington DC: United States Environmental Protection Agency* **1999**.
25. Emam, E. A.; Moawad, T. M.; Aboul-Gheit, N., Evaluating the characteristics of offshore oilfield produced water. *Petroleum & Coal* **2014,** 56, (4), 363-372.
26. Tang, G.-Q.; Morrow, N. R., Influence of brine composition and fines migration on crude oil/brine/rock interactions and oil recovery. *Journal of Petroleum Science and Engineering* **1999,** 24, (2), 99-111.
27. Tukey, J. W., Exploratory data analysis. **1977**.
28. Weiss, J.; Herrmann, N.; McClements, D., Ostwald ripening of hydrocarbon emulsion droplets in surfactant solutions. *Langmuir* **1999,** 15, (20), 6652-6657.
29. Hoang, T. K. N.; La, V. B.; Deriemaeker, L.; Finsy, R., Ostwald ripening of alkane emulsions stabilized by polyethylene glycol monolaurate. *Langmuir* **2001,** 17, (17), 5166-5168.
30. Sadtler, V. M.; Imbert, P.; Dellacherie, E., Ostwald ripening of oil-in-water emulsions stabilized by phenoxy-substituted dextrans. *Journal of colloid and interface science* **2002,** 254, (2), 355-361.
31. Moeini, F.; Hemmati-Sarapardeh, A.; Ghazanfari, M.-H.; Masihi, M.; Ayatollahi, S., Toward mechanistic understanding of heavy crude oil/brine interfacial tension: The roles of salinity, temperature and pressure. *Fluid phase equilibria* **2014,** 375, 191-200.
32. Abdel-Wali, A., Effect of simple polar compounds and salinity on interfacial tension and wettability of rock/oil/brine system effect. *Journal of King Saud University* **1996,** 8, 153-163.
33. Underwood, T. R.; Greenwell, H. C., The Water-Alkane Interface at Various NaCl Salt Concentrations: A Molecular Dynamics Study of the Readily Available Force Fields. *Scientific reports* **2018,** 8, (1), 352.
34. Shiu, W. Y.; Bobra, M.; Bobra, A. M.; Maijanen, A.; Suntio, L.; Mackay, D., The water solubility of crude oils and petroleum products. *Oil and Chemical pollution* **1990,** 7, (1), 57-84.
35. Voorhees, P. W., The theory of Ostwald ripening. *Journal of Statistical Physics* **1985,** 38, (1-2), 231-252.
36. Tadros, T. F., *Emulsion formation and stability*. John Wiley & Sons: 2013.
37. Wooster, T. J.; Golding, M.; Sanguansri, P., Impact of oil type on nanoemulsion formation and Ostwald ripening stability. *Langmuir* **2008,** 24, (22), 12758-12765.
38. Everett, D. H., *Basic principles of colloid science*. Royal society of chemistry: 2007.
39. Gupta, A.; Eral, H. B.; Hatton, T. A.; Doyle, P. S., Nanoemulsions: formation, properties and applications. *Soft Matter* **2016,** 12, (11), 2826-2841.
40. Gaweł, B.; Lesaint, C.; Bandyopadhyay, S.; Øye, G., Role of Physicochemical and Interfacial Properties on the Binary Coalescence of Crude Oil Drops in Synthetic Produced Water. *Energy & Fuels* **2015,** 29, (2), 512-519.

41. Veil, J. A.; Puder, M. G.; Elcock, D.; Redweik Jr, R. J., A white paper describing produced water from production of crude oil, natural gas, and coal bed methane. *Argonne National Laboratory, Technical Report* **2004,** 63.
42. Kokal, S. In *Crude oil emulsions: A state-of-the-art review*, SPE Annual Technical Conference and Exhibition, 2002; Society of Petroleum Engineers: 2002.
43. Hutin, A.; Argillier, J.-F.; Langevin, D., Influence of pH on Oil-Water Interfacial Tension and Mass Transfer for Asphaltenes Model Oils. Comparison with Crude Oil Behavior. *Oil & Gas Science and Technology–Revue d'IFP Energies nouvelles* **2016,** 71, (4), 58.
44. Chen, G.; Tao, D., An experimental study of stability of oil–water emulsion. *Fuel processing technology* **2005,** 86, (5), 499-508.
45. Guo, D.; Xie, G.; Luo, J., Mechanical properties of nanoparticles: basics and applications. *Journal of physics D: applied physics* **2013,** 47, (1), 013001.
46. Clasohm, L. Y.; Vakarelski, I. U.; Dagastine, R. R.; Chan, D. Y.; Stevens, G. W.; Grieser, F., Anomalous pH dependent stability behavior of surfactant-free nonpolar oil drops in aqueous electrolyte solutions. *Langmuir* **2007,** 23, (18), 9335-9340.
47. Erdlac Jr, R.; Armour, L.; Lee, R.; Snyder, S.; Sorensen, M.; Matteucci, M.; Horton, J. In *Ongoing resource assessment of geothermal energy from sedimentary basins in Texas*, Proceedings, thirty-second workshop on geothermal reservoir engineering, Stanford University, Stanford, SGP-TR-183, 2007; 2007.
48. Xin, S.; Liang, H.; Hu, B.; Li, K. In *Electrical power generation from low temperature co-produced geothermal resources at Huabei oilfield*, Proceedings, thirty-seventh workshop on geothermal reservoir engineering. Stanford University, Stanford, SGP-TR-194, 2012; 2012.
49. Cazabat, A.; Heslot, F.; Troian, S.; Carles, P., Fingering instability of thin spreading films driven by temperature gradients. *Nature* **1990,** 346, (6287), 824.
50. Israelachvili, J. N., *Intermolecular and surface forces: revised third edition*. Academic press: 2011.
51. Bennett, C. O.; Myers, J. E., *Momentum, heat, and mass transfer*. McGraw-Hill New York: 1962.
52. Binks, B. P.; Lumsdon, S. O., Stability of oil-in-water emulsions stabilised by silica particles. *Physical Chemistry Chemical Physics* **1999,** 1, (12), 3007-3016.
53. Depasse, J.; Watillon, A., The stability of amorphous colloidal silica. *Journal of Colloid and Interface Science* **1970,** 33, (3), 430-438.
54. Buenrostro‐Gonzalez, E.; Lira‐Galeana, C.; Gil‐Villegas, A.; Wu, J., Asphaltene precipitation in crude oils: Theory and experiments. *AIChE Journal* **2004,** 50, (10), 2552-2570.
55. Abdi, H.; Valentin, D., Multiple correspondence analysis. *Encyclopedia of measurement and statistics* **2007**, 651-657.
56. Ferragina, E.; Seeleib‐Kaiser, M.; Tomlinson, M., Unemployment protection and family policy at the turn of the 21st century: a dynamic approach to welfare regime theory. *Social Policy & Administration* **2013,** 47, (7), 783-805.
57. Taïeb, D.; Baumstarck-Barrau, K.; Sebag, F.; Fortanier, C.; De Micco, C.; Loundou, A.; Auquier, P.; Palazzo, F. F.; Henry, J.-f.; Mundler, O., Heath-related quality of life in thyroid cancer patients following radioiodine ablation. *Health and quality of life outcomes* **2011,** 9, (1), 33.